J|A|C|S COMMUNICATIONS

Published on Web 11/10/2010

Mechanism of H_2 Evolution from a Photogenerated Hydridocobaloxime

Jillian L. Dempsey, Jay R. Winkler,* and Harry B. Gray*

Beckman Institute, California Institute of Technology, Pasadena, California 91125, United States

Received October 17, 2010; E-mail: winklerj@caltech.edu; hbgray@caltech.edu

Abstract: Proton transfer from the triplet excited state of brominated naphthol to a difluoroboryl bridged Co^{I}-diglyoxime complex, forming $Co^{III}H$, was monitored via transient absorption. The second-order rate constant for $Co^{III}H$ formation is in the range $(3.5-4.7) \times 10^9$ M^{-1} s^{-1}, with proton transfer coupled to excited-state deactivation of the photoacid. $Co^{III}H$ is subsequently reduced by excess Co^{I}-diglyoxime in solution to produce $Co^{II}H$ ($k_{red} = 9.2 \times 10^6$ M^{-1} s^{-1}), which is then protonated to yield Co^{II}-diglyoxime and H_2.

The mechanisms of H_2 production catalyzed by molecular catalysts, like difluoroboryl bridged Co^{II}-diglyoxime complexes, are of great interest, as these catalysts are key elements in proposed solar-driven water splitting devices.[1] Among the most promising catalysts are those that rapidly evolve H_2 from acidic solutions, but in such cases it is difficult to observe catalytic intermediates by traditional spectroscopic methods. Several reaction mechanisms have been proposed that begin with protonation of a Co^{I} complex to form $Co^{III}H$; H_2 evolution can occur via protonation of $Co^{III}H$ or upon bimolecular combination of two $Co^{III}H$ species.[1] Alternatively, $Co^{III}H$ can be reduced further to form $Co^{II}H$, which can react via similar heterolytic or homolytic routes. We recently reported the laser flash-quench triggered reduction of a Co^{II}-diglyoxime species to Co^{I}.[2] In these experiments, time-resolved spectroscopy was used to detect the photochemically generated reduced species and monitor its reactivity. Analysis of these electron transfer reactions provided estimates of the barriers associated with the elementary steps in the proposed mechanistic cycles. Although reactivity through a homolytic route is favored, we were not able to obtain the kinetics of protonation and subsequent H_2 evolution steps with these transient techniques, as the strong acids needed for protonation caused catalyst degradation.

Here we describe an alternative technique based on excited-state proton transfer that has allowed us to trigger protonation of a Co^{I}-diglyoxime species and investigate the kinetics of catalytic H_2 evolution. Our approach employs photoacids that produce powerful proton donors upon excitation.[3−6] Although these pK_a jumps often are confined to the nanosecond lifetimes of singlet excited states, substitution with bromine facilitates intersystem crossing to generate high yields of long-lived triplet excited states, enabling bimolecular proton transfer reactions.[7,8] A case in point is the report of excited-state proton transfer from the triplet excited state of 6-bromo-2-naphthol (^{Br}NaphOH) to triethylamine in acetonitrile solution.[9]

We have observed excited-state proton transfer from ^{Br}NaphOH to a reduced cobaloxime, [Na][Co^{I}(dmgBF$_2$)$_2$(CH$_3$CN)] ([Na]**[Co^{I}]**), forming a hydride, HCo^{III}(dmgBF$_2$)$_2$(CH$_3$CN) (**[Co^{III}H]**), which subsequently reacts to produce H_2 (Scheme 1). In the ground state in acetonitrile solution, the pK_a of ^{Br}NaphOH is 26.1,[10,11] while the singlet and triplet excited states have pK_a values of approximately 13.7 and 14.6 (estimated from a Förster cycle),[3,12] respectively, which suggested that the photoacid would not react with [Na]**[Co^{I}]** in its ground state (see Supporting Information).

Scheme 1

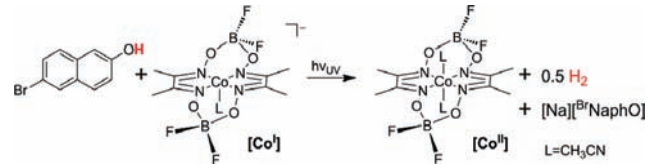

To test the reactivity of ^{3*}[^{Br}NaphOH] with **[Co^{I}]**, an acetontrile solution containing 672 μM ^{Br}NaphOH, 167 μM [Na]**[Co^{I}]**, and 100 mM [NBu$_4$][PF$_6$] was irradiated with 266 nm light in a 1 cm quartz cuvette. Absorption spectra measured at intervals indicated clean and quantitative conversion of **[Co^{I}]** to **[Co^{II}]**, confirmed by global analysis (see Supporting Information) and consistent with the overall reaction shown in Scheme 1. To confirm the production of H_2, bulk photolysis of a 40 mL stirring sample containing ~500 μM [Na]**[Co^{I}]**, 5 mM ^{Br}NaphOH, and 50 mM [NBu$_4$][PF$_6$] was performed in a custom 61 mL round-bottom flask fitted with a 1 in. diameter quartz window and a Teflon valve. After **[Co^{I}]** was converted to **[Co^{II}]**, monitored qualitatively via solution color change, the composition of the headspace gas was determined via gas chromatography. Quantifiable concentrations of H_2 were observed, with yields up to 64% based on the initial concentration of [Na]**[Co^{I}]**. Incomplete conversion is attributed to the GC detection limit as well as decomposition associated with the harsh conditions needed for photolysis of a concentrated solution.

With these results in hand, time-resolved measurements were carried out to monitor the proton transfer kinetics. Upon pulsed-laser excitation of ^{Br}NaphOH in the presence of [Na]**[Co^{I}]** (λ_{ex} = 266 nm, 3 mJ/pulse), we observed accelerated decay of the ^{3*}[^{Br}NaphOH] transient absorption (460 nm) attributable to excited-state proton transfer to form (**[Co^{III}H]**) and [Na][^{Br}NaphO]. Stern−Volmer quenching analysis yields a protonation rate constant (k_p) of 4.7×10^9 M^{-1} s^{-1} (Figure 1a). The consumption of **[Co^{I}]** upon protonation was monitored via single wavelength transient absorption at 630 nm (Figure 2). Two kinetics processes were observed, a fast reaction on the microsecond time scale followed by a slower reaction occurring over milliseconds (*vide infra*). The faster process is attributed to protonation of **[Co^{I}]** to form **[Co^{III}H]**, a species expected to have weak visible spectral features analogous to those of the yellow isolable Co^{III}CH$_3$ complex, MeCo^{III}(dmgBF$_2$)$_2$(CH$_3$CN) (see Supporting Information).[13] The fast kinetics phase best fit a single exponential decay plus a linear component to account for the slower decay process (Figure 2, top inset). The first-order rate constant for decay is linearly dependent on the concentration of **[Co^{I}]** under these pseudo-first-order conditions (cobaloxime in excess), giving a second-order rate constant for protonation (k_p) of 3.5×10^9 M^{-1} s^{-1} in agreement with the Stern−Volmer quenching analysis (Figure 1b).

The rate constant for protonation of **[Co^{I}]** by ^{3*}[^{Br}NaphOH] is a nearly diffusion-limited bimolecular process. Using digital simulations of cyclic voltammograms, Peters[14] and Fontecave[15] indepen-

10.1021/ja109351h

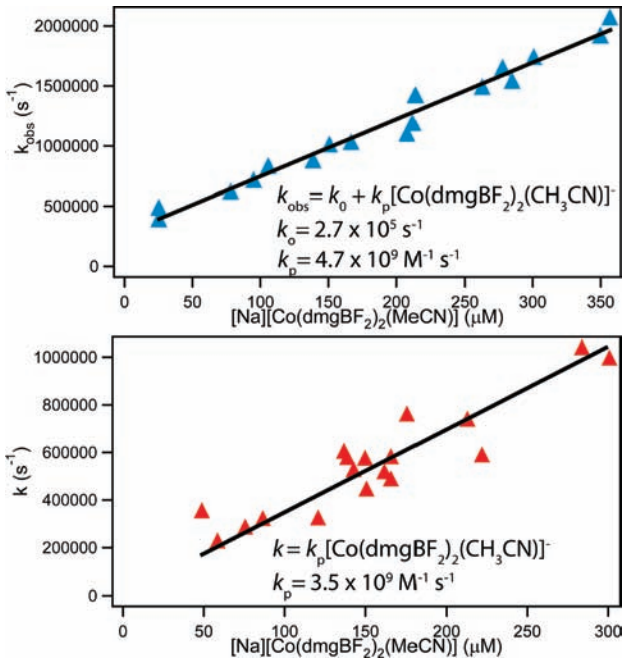

Figure 1. (a) First-order rate constants determined from excited-state quenching of 6-bromo-2-naphthol (λ_{ex} = 266 nm, λ_{obs} = 460 nm) in the presence of $[Co(dmgBF_2)_2(CH_3CN)]^-$. (b) First-order rate constants for bleaching $[Co(dmgBF_2)_2(CH_3CN)]^-$ absorption upon excitation of 6-bromo-2-naphthol (λ_{ex} = 266 nm, λ_{obs} = 630 nm). We found linear relationships between first-order rate constants and cobaloxime concentrations, allowing determination of a second-order rate constant for protonation.

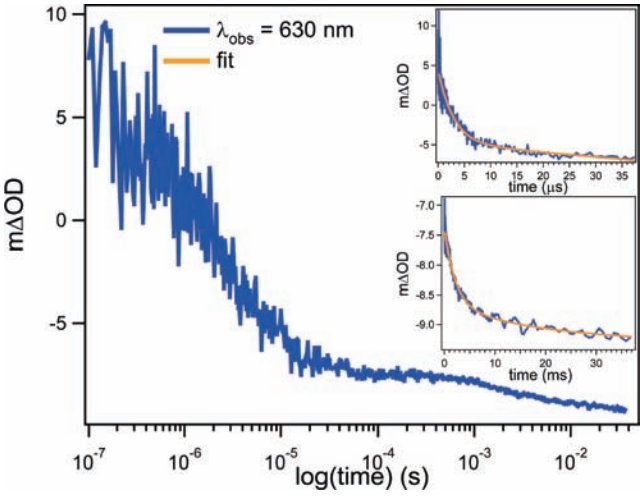

Figure 2. Typical transient kinetics trace for a sample containing 600 μM 6-bromo-2-naphthol, 50 μM [Na][Co^I(dmgBF$_2$)$_2$(CH$_3$CN)], and 100 mM [NBu$_4$][PF$_6$] in logarithmic time (λ_{obs} = 630 nm). Two sequential kinetics processes were observed. Insets: Kinetics traces and fits plotted on a linear time axis. The fast process (top) fits a single exponential plus linear decay kinetics; the slower reaction (bottom) fits biexponential kinetics.

dently estimated the rate constant for protonation of electrochemically generated **[Co^I]** by *p*-toluenesulfonic acid (pK_a = 8.0 in CH_3CN) and *p*-cyanoanilinium acid (pK_a = 7.6 in CH_3CN) to be between 7×10^3 and 1.5×10^5 M^{-1} s^{-1}. In related work, Bakac obtained a rate constant of 1.4×10^6 M^{-1} s^{-1} for reaction with citrate in neutral citrate buffered aqueous solution.[16] Based on the pK_a of 14.6 estimated for ^{3*}[^{Br}NaphOH], the measured rate constant for protonation is anomalously large compared to the aforementioned values. It is likely that proton transfer from ^{3*}[^{Br}NaphOH] to **[Co^I]** is coupled to deactivation of the excited state, leading to an increase in apparent acidity beyond the Förster value to a pK_a of −26.3, and accounting for the very high observed rate constant. Tetrabutylammonium tosylate, the conjugate base of *p*-toluenesulfonic acid, quenches ^{3*}[^{Br}NaphOH], consistent with this much lower pK_a value (see Supporting Information).

In the electrochemical analysis by Peters and co-workers,[14] protonation was found to be rate limiting for catalysis. In our work, however, the rapid rate of protonation allows the kinetics of subsequent steps to be monitored. The slower process observed in transient measurements at 630 nm is best fit to a biexponential decay (Figure 2, bottom inset). When the concentration of **[Co^I]** is varied, the rate constant for the faster component varies linearly while the second rate constant ($k \approx 100\ s^{-1}$) is independent of concentration. The plot of the observed first-order rate constant for the faster process versus **[Co^I]** concentration gives a second-order rate constant of 9.2×10^6 M^{-1} s^{-1} (see Supporting Information).

Concurrent with the bleach of the **[Co^I]** signal, a new absorption feature was observed in transient measurements between 380 and 450 nm. Attempts to obtain kinetics of formation of this intermediate were not successful, owing to the intense absorption of ^{3*}[^{Br}NaphOH] in this spectral region. On longer time scales, a transient signal monitored at 405 nm (Figure 3) decays to a more weakly absorbing final product, **[Co^{II}]**. The conversion is best fit to single exponential decay with a rate constant of ∼100 s^{-1}, matching the slowest kinetics process from 630 nm traces. Additional experiments revealed that the first-order rate constant for decay of this intermediate (monitored at 405 nm) scales linearly with the concentration of ^{Br}NaphOH, giving a second-order rate constant of 4.2×10^4 M^{-1} s^{-1}.

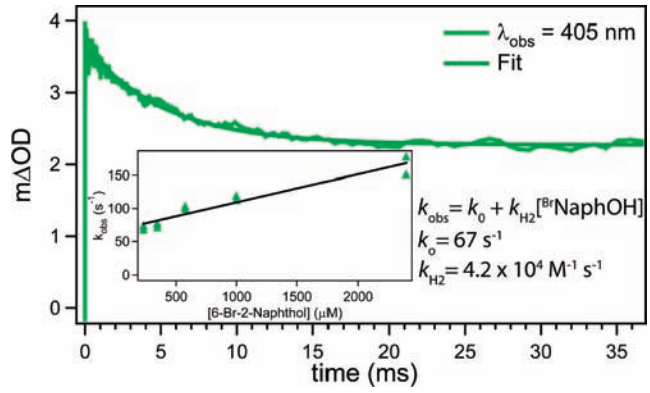

Figure 3. Typical transient kinetics trace at 405 nm for a sample containing 583 μM 6-bromo-2-naphthol, 263 μM [Na][Co^I(dmgBF$_2$)$_2$(CH$_3$CN)], and 100 mM [NBu$_4$][PF$_6$] fits single exponential decay. Inset: Linear relationship between first-order rate constants for decay at 405 nm and the concentration of 6-bromo-2-naphthol allows estimation of a second-order rate constant for H_2 release. Conditions: ∼80 μM [Na][Co^I(dmgBF$_2$)$_2$(CH$_3$CN)] and 100 mM [NBu$_4$][PF$_6$].

The transient absorption measurements are consistent with the kinetics model outlined in Scheme 2. Electronic excitation of ^{Br}NaphOH promotes excited-state proton transfer to **[Co^I]**, forming **[Co^{III}H]**. The second kinetics phase correlates with reduction of transiently generated **[Co^{III}H]** by excess **[Co^I]** to form a reduced hydride species, $[HCo^{II}(dmgBF_2)_2(CH_3CN)]^-$ (**[Co^{II}H]**) and **[Co^{II}]**. The **[Co^{II}H]** transient is a strongly absorbing yellow species with a weak spectral feature at 630 nm. Protonation of this intermediate by weakly acidic ^{Br}NaphOH releases H_2 and generates **[Co^{II}]** (k_{H_2} = 4.2×10^4 M^{-1} s^{-1}), indicating that **[Co^{II}H]** is strongly hydridic.[17] A similar heterolytic route proceeding via **[Co^{II}H]** likely is the dominant pathway in photocatalytic H_2 evolution reactions reported by Eisenberg[18−21] and Fontecave,[22] where experimental conditions

Scheme 2

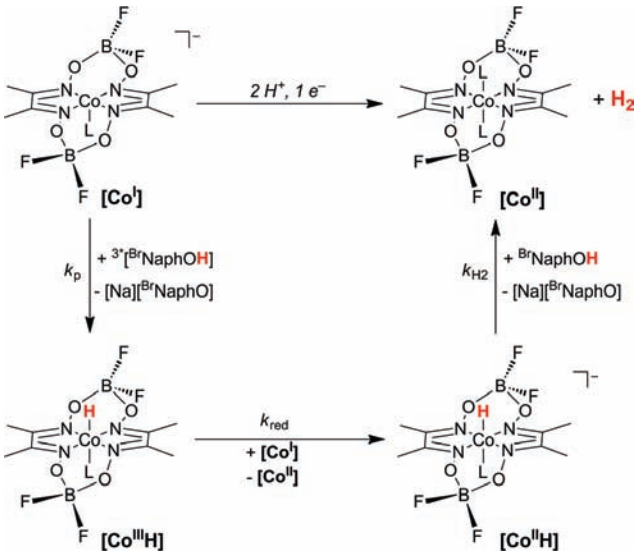

included both weakly basic solutions and high concentrations of powerful reductants.

The rate constant for reduction of **[Co^{III}H]** by **[Co^{I}]** (k_{red} = 9.2 × 10^6 M^{-1} s^{-1}) corresponds to a barrier of 5−7 kcal mol^{-1} (see Supporting Information). The work of Peters and co-workers is relevant here, as a quasi-reversible reduction peak in their cyclic voltammograms attributable to **[Co^{III}H]**/**[Co^{II}H]** reduction was observed ∼0.45 V negative of the **[Co^{II}]**/**[Co^{I}]** reduction potential, implying a lower limit of ∼10.5 kcal mol^{-1} for the barrier to this reduction.[14] Our work suggests that **[Co^{III}H]** is more readily reduced than previously thought.

Chao and Espenson obtained a second-order rate constant of 1.7 × 10^4 M^{-1} s^{-1} for H_2 production from an isolable phosphine stabilized hydride species, $HCo(dmgH)_2P(n\text{-}C_4H_9)_3$ ([PCo^{III}H]),[23] a value that corresponds to a barrier of approximately 8−10 kcal mol^{-1} for bimolecular reductive elimination. As the hydride of the cobaloxime explored here (**[Co^{III}H]**) is more reactive,[14] a reasonable estimate for the analogous homolytic barrier would be 5−8 kcal mol^{-1}, similar to that observed for the reduction of **[Co^{III}H]**. However, under our experimental conditions, the concentration of **[Co^{I}]** is significantly greater than that of the transiently generated **[Co^{III}H]**. Thus a pathway in which the hydride is further reduced is favored.

We have demonstrated that photoacid triplet excited states can rapidly trigger protonation of metal complexes. Our work suggests that protonation of **[Co^{I}]** by ^{3*}[^{Br}NaphOH] is coupled to excited-state deactivation. The rapid rate of protonation has allowed us to study subsequent processes. Importantly, we found that transiently generated **[Co^{III}H]** is reduced by **[Co^{I}]** to form **[Co^{II}H]**, which is then protonated by ^{Br}NaphOH to generate 1 equiv of H_2 and **[Co^{II}]**. Our experiments have revealed a hydrogen evolution pathway via protonation of **[Co^{II}H]** that is expected to dominate when low concentrations of **[Co^{III}H]** and an excess of reducing equivalents are present.

Acknowledgment. We thank Bruce Brunschwig, Alec Durrell, Maraia Ener, Jonas Peters, and Jeff Warren for helpful discussions and experimental advice. Charles McCrory and Jacob Good are acknowledged for generous assistance with GC measurements. This work was supported by an NSF Center for Chemical Innovation (Powering the Planet, CHE-0947829), the Arnold and Mabel Beckman Foundation, and CCSER (Gordon and Betty Moore Foundation). J.L.D. was supported by an NSF Graduate Research Fellowship.

Supporting Information Available: Full details of synthesis, photochemical experiments, transient and steady-state absorption measurements, global analysis, and bulk photolysis. This information if available free of charge via the Internet at http://pubs.acs.org.

References

(1) Dempsey, J. L.; Brunschwig, B. S.; Winkler, J. R.; Gray, H. B. *Acc. Chem. Res.* **2009**, *42*, 1995–2004.
(2) Dempsey, J. L.; Winkler, J. R.; Gray, H. B. *J. Am. Chem. Soc.* **2010**, *132*, 1060–1065.
(3) Forster, T. *Z. Elektrochem.* **1950**, *54*, 531–535.
(4) Tolbert, L. M.; Solntsev, K. M. *Acc. Chem. Res.* **2001**, *35*, 19–27.
(5) Arnaut, L. G.; Formosinho, S. J. *J. Photochem. Photobiol. A* **1993**, *75*, 1–20.
(6) Gutman, M.; Huppert, D. *J. Biochem. Biophys. Methods* **1979**, *1*, 9–19.
(7) McClure, D. S. *J. Chem. Phys.* **1949**, *17*, 905–913.
(8) McClure, D. S.; Blake, N. W.; Hanst, P. L. *J. Chem. Phys.* **1954**, *22*, 255–258.
(9) Pretali, L.; Doria, F.; Verga, D.; Profumo, A.; Freccero, M. *J. Org. Chem.* **2009**, *74*, 1034–1041.
(10) Bordwell, F. G.; Cheng, J. *J. Am. Chem. Soc.* **1991**, *113*, 1736–1743.
(11) Kütt, A.; Leito, I.; Kaljurand, I.; Sooväli, L.; Vlasov, V. M.; Yagupolskii, L. M.; Koppel, I. A. *J. Org. Chem.* **2006**, *71*, 2829–2838.
(12) Grabowski, Z. R.; Rubaszewska, W. *J. Chem. Soc., Faraday Trans. 2* **1977**, *73*, 11–28.
(13) Ram, M. S.; Riordan, C. G.; Yap, G. P. A.; LiableSands, L.; Rheingold, A. L.; Marchaj, A.; Norton, J. R. *J. Am. Chem. Soc.* **1997**, *119*, 1648–1655.
(14) Hu, X.; Brunschwig, B. S.; Peters, J. C. *J. Am. Chem. Soc.* **2007**, *129*, 8988–8998.
(15) Baffert, C.; Artero, V.; Fontecave, M. *Inorg. Chem.* **2007**, *46*, 1817–1824.
(16) Szajna-Fuller, E.; Bakac, A. *Eur. J. Inorg. Chem.* **2010**, *2010*, 2488–2494.
(17) Curtis, C. J.; Miedaner, A.; Ellis, W. W.; DuBois, D. L. *J. Am. Chem. Soc.* **2002**, *124*, 1918–1925.
(18) Du, P.; Knowles, K.; Eisenberg, R. *J. Am. Chem. Soc.* **2008**, *130*, 12576–12577.
(19) Du, P.; Schneider, J.; Luo, G.; Brennessel, W. W.; Eisenberg, R. *Inorg. Chem.* **2009**, *48*, 4952–4962.
(20) Lazarides, T.; McCormick, T.; Du, P.; Luo, G.; Lindley, B.; Eisenberg, R. *J. Am. Chem. Soc.* **2009**, *131*, 9192–9194.
(21) McCormick, T. M.; Calitree, B. D.; Orchard, A.; Kraut, N. D.; Bright, F. V.; Detty, M. R.; Eisenberg, R. *J. Am. Chem. Soc.* **2010**, *132*, 15480−15483.
(22) Fihri, A.; Artero, V.; Pereira, A.; Fontecave, M. *Dalton Trans.* **2008**, 5567–5569.
(23) Chao, T.-H.; Espenson, J. H. *J. Am. Chem. Soc.* **1978**, *100*, 129–133.

JA109351H